

Ultra-Low Loss 698 nm and 450 nm Silicon Nitride Visible Wavelength Waveguides for Strontium Atomic Clock Applications

Nitesh Chauhan, Jiawei Wang, Debapam Bose, Renan Moreira, Daniel J. Blumenthal

¹ Department of Electrical and Computer Engineering, University of California Santa Barbara
danb@ucsb.edu

Abstract: We report tightly confining Si₃N₄ waveguides with record low loss at key strontium clock visible wavelengths, 0.03dB/cm at $\lambda=698\text{nm}$, 0.08dB/cm at 450nm and ring resonators with measured loaded Q of 8.6 million at $\lambda=674\text{nm}$. © 2020 The Author(s)

OCIS codes: (230.7390) waveguides, planar; (250.5300) photonic integrated circuits.

1. Introduction

Photonic integrated circuits with ultra-low losses ($< 0.1 \text{ dB/cm}$) in the visible region are critical for miniaturizing atom based quantum communication [1], information processing systems [2], and optical atomic clocks [3]. Today, these systems employ free-space beam delivery with complex optical systems that occupy racks and tabletops. Photonic integration is the next key step to reduction in size and complexity paving the way for compact low power, low cost systems. Recent efforts to integrate laser beam delivery at visible wavelengths include low loss Al₂O₃ and Si₃N₄ [4-6] waveguides. Si₃N₄ is transparent from 405nm-2350nm [7] and has been used for devices at telecom wavelength (1550nm) [8–10] and as well as visible applications [7] including recent laser cooling beam delivery interface for 780nm rubidium atom clock applications [11]. While low loss IR and near IR (NIR) Si₃N₄ waveguides have been demonstrated [5], progress in ultra-low-loss Si₃N₄ waveguides at visible wavelengths in the 450 nm to 700 nm, wavelengths of interest for many atomic systems including strontium, has been limited.

In this paper we report ultra-low loss waveguides operating from the blue to NIR fabricated in a CMOS compatible Si₃N₄ platform [8-12]. We measured record low losses of 0.03dB/cm at $\lambda=698\text{nm}$ and 0.08dB/cm at $\lambda=450\text{nm}$ over 2m long waveguide spirals. We demonstrate spiral waveguides with a core geometry of 20nm thick and 2.3 μm wide with a critical bend radius of 3.5mm for $\lambda=698\text{nm}$ and 20nm thick and 1.3 μm wide with a critical bend radius of 400 μm at $\lambda=450\text{nm}$. A second core geometry with the thickness of 90nm suitable for compact devices from red to near infrared at the cost of higher propagation loss is also demonstrated. We designed polarization selective S bends, inverted taper spot size converters at facet for mode matching in both core geometries. We also fabricate and measure a record high 8.6 million Q, for a visible wavelength bus waveguide coupled, all-pass ring resonator with a radius of 9610.66 μm , Si₃N₄ core thickness of 20nm, waveguide width of 2.3 μm and 2.25 μm gap with 4.55% coupling coefficient, operating at a strontium resonant wavelength of 674 nm.

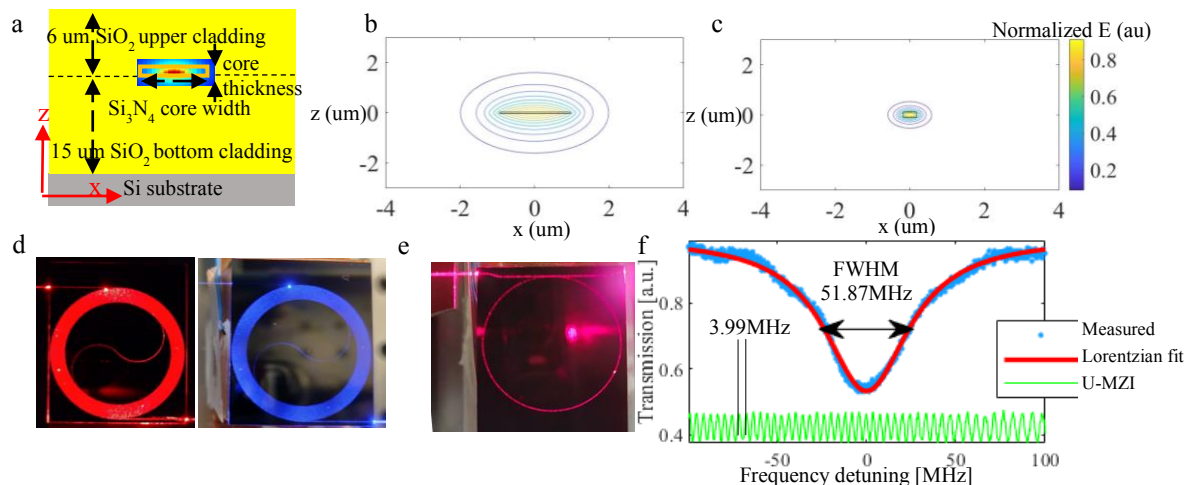


Figure 1 (a) Waveguide Cross section (b) mode profile for $\lambda=698\text{nm}$ in 20nm thick, 2.3 μm wide waveguide showing a large dilute mode (c) mode profile for $\lambda=698\text{nm}$ in 90nm thick, 400nm wide waveguide showing a small highly confined mode (d) 2m spirals in 20 nm core with 698nm and 450nm light coupled into the spiral (e) all pass ring resonator with 674nm light coupled into the bus (f) Q measurement of all pass ring resonator with measured loaded Q of 8.6 million.

Our waveguides support both TE and TM modes in straight sections but only TE modes in bends due to high TM loss. We demonstrate both multi-S bend designs and spiral designs. Both designs are single polarization mode [12]. The waveguide modes are shown in figure 1 (b) and (c) for $\lambda=698\text{nm}$ for the two core geometries. A 20 nm thick core has smaller waveguide cross section but much larger mode volume. This reduces mode overlap with waveguide core area and leads to a reduction in loss contributed by core material absorption. Also, the roughness of the waveguide sidewalls is over a magnitude higher than roughness of top and bottom surface of deposited film [9]. A thinner core, 20nm in our case, has much smaller contribution of loss from sidewall roughness as compared to a thicker 90nm core. The 90 nm thick waveguide core geometry is ideal for applications where compact structures are required, for instance, we have demonstrated large area grating at $\lambda=780\text{nm}$ in this core [11]. For red and near infrared wavelengths, 90nm core offers better compromise for compact structures and 20nm can be selected for applications low loss is critical for operation. The waveguide fabrication process is same as in [8].

2. Results

We measure the fiber to waveguide coupling losses in straight waveguides. For 20nm core, we made 2m concentric spirals with widths of 2.3 μm and 1.3 μm for $\lambda=698\text{nm}$ and $\lambda=450\text{nm}$, respectively, as shown in Table 1. The minimum bend radii of these were designed as 3.5mm so that there is no contribution of bend loss. These were used to measure the total loss, and the coupling loss from straight waveguides was deducted to get the propagation loss. The coupling losses were found to be $4.7\pm 0.2\text{dB/facet}$ and $3\pm 0.4\text{dB/facet}$. The propagation losses were 0.03dB/cm at $\lambda=698\text{nm}$ and 0.08dB/cm at $\lambda=450\text{nm}$. The variation in loss over all devices were $\pm 0.008\text{dB/cm}$ at $\lambda=698\text{nm}$ and $\pm 0.01\text{dB/cm}$ at $\lambda=450\text{nm}$. For 90nm core, we designed cutback spirals of three different lengths, 0.5m, 1m and 1.5m to measure loss at $\lambda=698\text{nm}$ and $\lambda=808\text{nm}$. We used cutback method on straight waveguides for losses at $\lambda=450\text{nm}$ in 90nm core. Table 1 summarizes waveguide geometries and their corresponding losses.

The Q was measured using a calibrated unbalanced MZI as in [8] with fringe width 3.99MHz. The measured FWHM for ring resonator is 51.87MHz with loaded Q of 8.6 million at $\lambda=674\text{nm}$. Calculating loss from Q value yields 0.036dB/cm which matches well with loss measured through spirals. Such low loss will enable high Q resonator-based devices like Brillouin lasers, low loss delay lines, directional couplers and efficient gratings in visible region to move discrete free space components to PICs.

Table 1. Summary of losses and waveguide geometries

	Parameters	$\lambda=450\text{nm}$	$\lambda=698\text{nm}$	$\lambda=808\text{nm}$	
Core thickness 90 nm	Core width	0.3	0.4	0.4	μm
	Propagation loss	5.065	0.2422	0.1262	dB/cm
	Coupling loss	6	3.0*	2.7*	dB/facet
Core thickness 20 nm	Core width	1.3	2.3	----	μm
	Propagation loss	0.08	0.03	----	dB/cm
	Coupling loss	3	4.5	----	dB/facet
	Loaded Q	----	8.6×10^6 (674nm)	----	

* with inverted taper spot size converter

3. Acknowledgements and Funding information: This work was supported by DARPA MTO APhI contract number FA9453-19-C-0030. The views, opinions, and/or findings expressed are those of the authors and should not be interpreted as representing the official views or policies of the Department of Defense or the U.S. Government.

4. References

- [1] I. Bloch, *Nature*, vol. 453, no. 7198, pp. 1016–1022, Jun. 2008.
- [2] T. D. Ladd *et al.*, *Nature*, vol. 464, no. 7285, pp. 45–53, Mar. 2010.
- [3] A. D. Ludlow *et al.*, *Rev. Mod. Phys.*, vol. 87, no. 2, pp. 637–701, Jun. 2015.
- [4] K. K. Mehta *et al.*, *Nature Nanotechnology*, vol. 11, no. 12, pp. 1066–1070, Dec. 2016.
- [5] S. Bramhavar *et al.*, *Integrated Optics: Devices, Materials, and Technologies XXIII*, 2019, vol. 10921, p. 109211D.
- [6] M. T. Hummon *et al.*, *Optica*, vol. 5, no. 4, p. 443, Apr. 2018.
- [7] D. J. Blumenthal *et al.*, *Proceedings of the IEEE*, vol. 106, no. 12, pp. 2209–2231, Dec. 2018.
- [8] S. Gundavarapu *et al.*, *Nature Photon*, vol. 13, no. 1, pp. 60–67, Jan. 2019.
- [9] J. F. Bauters *et al.*, in *37th European Conference and Exposition on Optical Communications*, Geneva, 2011, p. Th.12.LeSaleve.3.
- [10] M. Belt *et al.*, *Opt. Express*, *OE*, vol. 21, no. 1, pp. 1181–1188, Jan. 2013.
- [11] N. Chauhan *et al.*, in *Conference on Lasers and Electro-Optics (2019)*, paper STu4O.3, 2019, p. STu4O.3.
- [12] J. F. Bauters *et al.*, *IEEE Photonics Journal*, vol. 5, no. 1, pp. 6600207–6600207, Feb. 2013.